



ELSEVIER

Journal of Non-Crystalline Solids 287 (2001) 135–139

JOURNAL OF
NON-CRYSTALLINE SOLIDS

www.elsevier.com/locate/jnoncrysol

The magnetic and structural properties of the high-coercivity $\text{Nd}_{50}\text{Fe}_{40}\text{Al}_{10}$ amorphous alloys

Horia Chiriac*, N. Lupu

National Institute of Research and Development for Technical Physics, 47 Mangeron Blvd., R-6600 Iasi, Romania

Abstract

Melt-spun amorphous ribbons with thicknesses between 25 and 150 μm and amorphous rods with diameters between 0.5 and 2 mm, prepared by copper mould suction casting, having nominal composition $\text{Nd}_{50}\text{Fe}_{40}\text{Al}_{10}$, were measured. The magnetic properties were measured as a function of temperature from 5 to 800 K. The dependence of the coercive field on the thickness of the samples and temperature is ascribed to two magnetic phases: Fe–Nd ferromagnetic clusters and a Nd-based matrix. The differences observed between zero-field-cooled (M_{ZFC}) and field-cooled (M_{FC}) magnetisations as well as the presence of a cusp on the M_{ZFC} curve, and its displacement as a function of the magnitude of the external field are consistent with two types of magnetic order: spin-glass-like short-range order and long-range ferromagnetic order. © 2001 Elsevier Science B.V. All rights reserved.

PACS: 75.50.Kj

1. Introduction

The magnetism of rare earth (RE)–Fe glassy alloys, produced by quenching from the liquid has been studied [1,2]. More recently, the magnetic and structural properties of melt-spun Nd–Fe and Pr–Fe alloys close to the eutectic have been investigated. A new glassy or nanocrystalline phase (crystalline phase is in nanometer size crystals) of approximate composition Fe_3RE , so-called A_1 phase, responsible for the coercivity observed at room temperature was proposed [3]. It is known [4] that the addition of Al to Nd–Fe–B intermetallic compounds increases the coercivity by modifying the microstructure. Moreover, it has been found [5] that the addition of Al to RE–Fe

binary alloys makes possible the preparation of thicker amorphous samples by a mould casting method. $\text{Nd}_{60}\text{Fe}_{30}\text{Al}_{10}$ amorphous samples have harder magnetic properties at room temperature differing from ribbons prepared from the same alloy, which are magnetically soft [6].

In this paper some results concerning the investigation of several $\text{Nd}_{50}\text{Fe}_{40}\text{Al}_{10}$ melt-spun amorphous ribbons and cast rods, both of them with coercivities larger than 100 kA/m at room temperature, are presented. We considered the glass formation phenomena, magnetic properties and their dependence on temperature and the relationship between microstructure and magnetic properties.

2. Experimental

The $\text{Nd}_{50}\text{Fe}_{40}\text{Al}_{10}$ master alloy was prepared from Fe (99.99%), Nd (99.9%) and Al (99.99%) in

* Corresponding author. Tel.: +40-32 130 680; fax: +40-32 231 132.

E-mail address: hchiriac@phys-iasi.ro (H. Chiriac).

an arc furnace under Ar atmosphere, and re-melted several times for homogenisation. Ribbons with thicknesses between 25 and 150 μm and widths of 3 up to 5 mm were obtained by single roller melt-spinning method in vacuum or in Ar atmosphere, at surface velocities of the Cu wheel ranging between 30 and 5 m/s. Rods with diameters between 0.5 and 2 mm were prepared by copper mould suction casting method in an Ar atmosphere. The master alloy was melted in a water cooled copper mould in arc melting chamber and suction thereafter in another cooled mould with different internal diameters by applying a sucking pressure (about 1 atm) at the bottom part of this mould. All the samples were determined to be non-crystalline by X-ray diffraction. The thermal stability associated with crystallisation and melting temperature was measured by differential scanning calorimetry (DSC). Magnetisation measurements above room temperature, at applied magnetic fields limited to 0.8 T, were carried out using a vibrating sample magnetometer (VSM). The magnetisation and coercive field below room temperature were studied using a superconducting quantum interference device (SQUID) Magnetometer. Each sample was thermally demagnetised prior to recording each measurement. Zero-field-cooled magnetisation (M_{ZFC}) was measured on heating in applied field after cooling to 0°C in zero applied field, while the field-cooled magnetisation (M_{FC}) was measured during warming in applied field after the field cooling.

3. Results

Fig. 1 illustrates the DSC curves for $\text{Nd}_{50}\text{Fe}_{40}\text{Al}_{10}$ melt-spun ribbons with thicknesses between 25 and 142 μm , recorded at a heating rate of 0.67 K/s. DSC curves have one exothermic peak which we attribute to the crystallisation process for the entire range of thicknesses indicating that the samples does not contain crystalline phases, in agreement with the XRD measurements [7]. Neither endothermic reaction due to the glass transition nor the supercooled liquid region in the temperature range before crystallisation is seen on the DSC curves. Therefore, the glass-forming

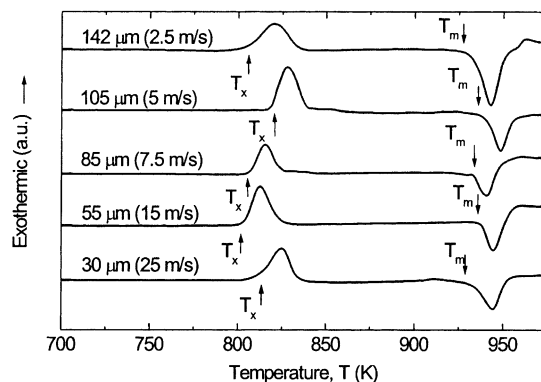


Fig. 1. DSC curves of the $\text{Nd}_{50}\text{Fe}_{40}\text{Al}_{10}$ amorphous ribbons with different thicknesses (in bracket are the corresponding wheel velocities).

ability of $\text{Nd}_{50}\text{Fe}_{40}\text{Al}_{10}$ amorphous alloy is determined by the reduced temperature T_x/T_m , where T_x and T_m represent the crystallisation and eutectic melting temperature, respectively.

In Fig. 2 are presented hysteresis loops at room temperature as a function of the thickness of the $\text{Nd}_{50}\text{Fe}_{40}\text{Al}_{10}$ amorphous ribbons and rods. An increase of the thickness results in the increase of the coercive field by about four times, from 65 kA/m for the ribbon having 30 μm in thickness to about 240 kA/m for the ribbon having 142 μm . The increase of the amorphous ribbons' thickness decreases the magnetisation. The coercive field is about 200 kA/m for $\text{Nd}_{50}\text{Fe}_{40}\text{Al}_{10}$ amorphous rods, regardless of their diameter. For comparison, in inset are presented the hysteresis loops plotted

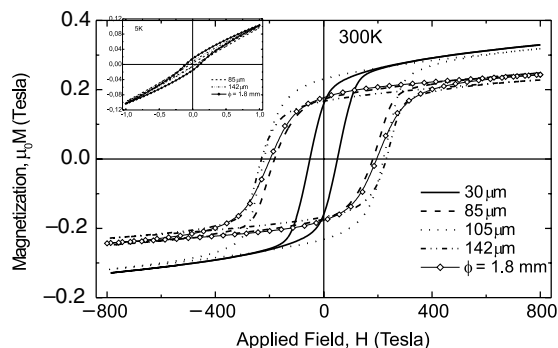


Fig. 2. Hysteresis loops plotted at room temperature and 5 K (inset) for $\text{Nd}_{50}\text{Fe}_{40}\text{Al}_{10}$ amorphous ribbons and rods.

at 5 K. We note that while for $\text{Nd}_{50}\text{Fe}_{40}\text{Al}_{10}$ amorphous ribbons there is no hysteresis, the magnetisation of $\text{Nd}_{50}\text{Fe}_{40}\text{Al}_{10}$ amorphous rods have hysteresis loop that we deconvolute in one sigmoidal loop associated with the magnetic response of the Nd-rich magnetic phase and one square loop due to the Fe–Nd hard magnetic phase [8].

The variation of the magnetic properties with temperature below room temperature, i.e., magnetisation measured at a maximum applied magnetic field of 1 T and intrinsic coercive field, is presented in Fig. 3. We observe that for $\text{Nd}_{50}\text{Fe}_{40}\text{Al}_{10}$ amorphous ribbons the magnetisation decreases with temperature, attains a minimum at about 100 K, then increases about seven times at lower temperatures. The magnetisations of the amorphous rods increase continuously with increasing temperature. The coercive field has an increase for $\text{Nd}_{50}\text{Fe}_{40}\text{Al}_{10}$ amorphous rods, amounting to about 550 kA/m at 200 K. For ribbons, in the temperature range 5–100 K the coercive field is smaller, practically there is no

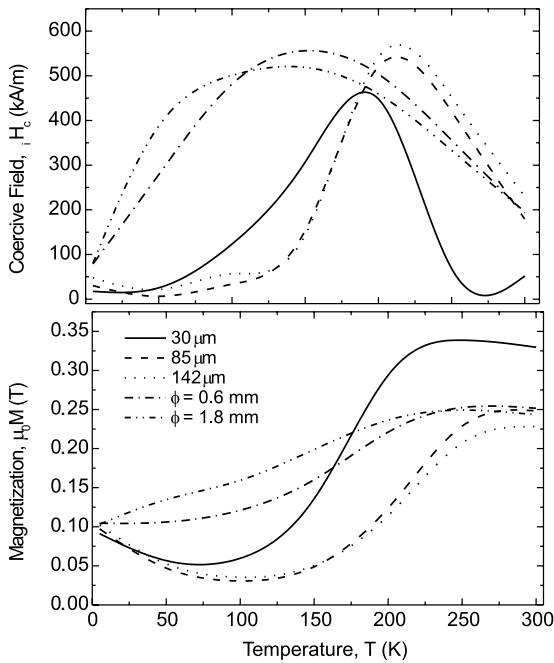


Fig. 3. The variation of the magnetic properties as a function of temperature for $\text{Nd}_{50}\text{Fe}_{40}\text{Al}_{10}$ amorphous ribbons and rods.

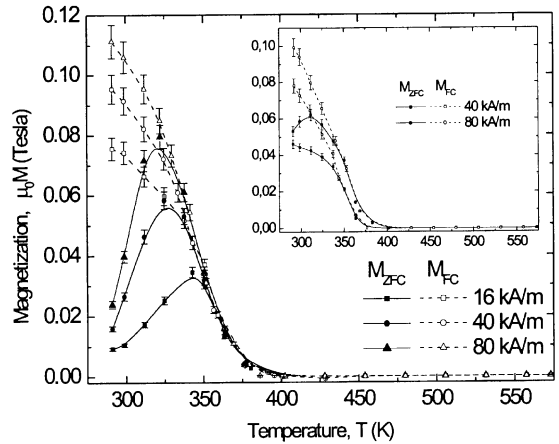


Fig. 4. M_{ZFC} and M_{FC} curves for $\text{Nd}_{50}\text{Fe}_{40}\text{Al}_{10}$ amorphous ribbons 85 μm in thickness and amorphous rods 1.8 mm in diameter (inset) (lines are drawn as a guide to the eye).

hysteresis loop. At around 200 K the coercive field increases and reaches 450 to about 600 kA/m for thicknesses ranging from 30 to 142 μm . This specific change of the magnetic properties at temperatures below 200 K we ascribe to the presence of Fe–Nd ferromagnetic clusters embedded in Nd-rich matrix, whose dynamics change with increasing temperature. Another evidence of the existence of two types of magnetic order are the M_{ZFC} and M_{FC} curves above room temperature, plotted in Fig. 4 for $\text{Nd}_{50}\text{Fe}_{40}\text{Al}_{10}$ amorphous ribbon 85 μm in thickness and $\text{Nd}_{50}\text{Fe}_{40}\text{Al}_{10}$ amorphous rods 1.8 mm in diameter (inset) as well as the modification of the hysteresis loops by annealing the thin rib-

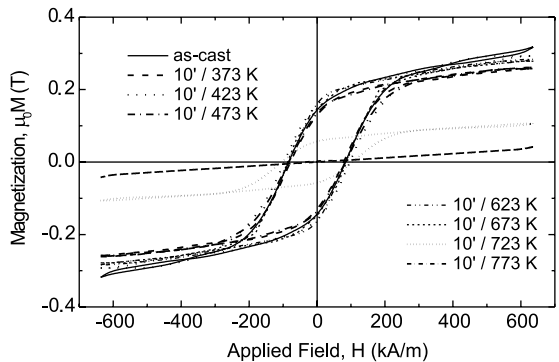


Fig. 5. Hysteresis loops as a function of annealing temperature for $\text{Nd}_{50}\text{Fe}_{40}\text{Al}_{10}$ amorphous ribbon 30 μm in thickness.

bons at temperatures less than and greater than crystallisation temperature (about 713 K) presented in Fig. 5.

4. Discussion

From Fig. 1 we observe that the largest reduced temperature T_x/T_m of about 0.873 is obtained for the $\text{Nd}_{50}\text{Fe}_{40}\text{Al}_{10}$ amorphous ribbon with a thickness of 105 μm indicating that for this thickness structure was the most disordered [7]. This disorder is confirmed by the fact that this ribbon has also larger magnetisation and coercive field.

The dependence of the intrinsic coercive field on the thickness of the $\text{Nd}_{50}\text{Fe}_{40}\text{Al}_{10}$ amorphous samples, namely the quench rate, we ascribe to the existence of two magnetic phases in the amorphous structural phase. One of them consists in Fe–Nd ferromagnetic clusters coupled inside and between them by ferromagnetic exchange interactions and the other is the Nd-rich matrix in which are embedded the clusters [9]. The hysteresis loop at room temperature is the response of the magnetic cluster phase, because the Nd-rich phase is paramagnetic and makes no contribution. The annealing at temperatures less than crystallisation temperature, as shown in Fig. 5, leaves almost unchanged the magnetic properties, which we suggest is due to the thermal stability of this amorphous alloy in a range of temperatures. The onset of the crystallisation process forms one metastable phase, which has larger coercive field but smaller magnetisation in comparison with the amorphous phase. This metastable phase disappears after annealing at 773 K, above this temperature the sample becoming paramagnetic.

From the hysteresis loops plotted at 5 K and from the variation of the magnetisation and coercive field with temperature in the range 5–300 K we observed that at lower temperatures several magnetic phase transitions take place. At temperatures less than 70 K the large anisotropy of the Nd^{3+} ions is randomly oriented, which dominates the magnetisation of each Fe–Nd [10]. By increasing the temperature the exchange interactions between clusters become more and more important. At temperatures higher than 150 K the

thermal activation processes increase and the magnetic response is a result of the competition between the thermal effects and magnetic exchange interactions [11].

We note that the glassy structure in the $\text{Nd}_{50}\text{Fe}_{40}\text{Al}_{10}$ amorphous rods prepared by copper mould suction casting is more relaxed because of the smaller quench rate ($\approx 10^2$ K/s), in comparison with the quench rates of the melt-spinning method ($\approx 10^5$ K/s).

The cusp in the M_{ZFC} magnetisation curves (see Fig. 4), whose position changes with decreasing temperatures by increasing the magnitude of the external field, and the bifurcation of the M_{ZFC} and M_{FC} curves are characteristic of systems in which ferromagnetic long-range order and spin-glass or cluster-glass short-range order exist [12]. The same changes were observed for both $\text{Nd}_{50}\text{Fe}_{40}\text{Al}_{10}$ amorphous ribbons and rods, the only differences being observed for the position of the cusp as a function of the amorphous ribbons' thickness and being related to the thermal effect [13].

5. Conclusions

$\text{Nd}_{50}\text{Fe}_{40}\text{Al}_{10}$ amorphous alloys have coercive fields for both melt-spun ribbons and suction cast rods. The coercive field increases with decreasing temperature attaining about 600 kA/m around 200 K. Its increase with the increase of the amorphous samples' thickness and the dependence on the quench rate and the preparation process are related to the existence of two magnetic phases in the amorphous structure: Fe–Nd ferromagnetic coupled clusters and Nd-rich phase. The bifurcation of the M_{ZFC} and M_{FC} curves as well as the existence of the cusp on the M_{ZFC} curve is a proof of the coexistence of spin-glass short-range order and long-range ferromagnetic order. The magnetic properties as a function of temperature and thermomagnetic history of the $\text{Nd}_{50}\text{Fe}_{40}\text{Al}_{10}$ amorphous alloys as well as the thermal stability of the magnetic properties in a range of temperatures make these alloys interesting both from fundamental research point of view and for their applications.

References

- [1] R.C. Taylor, T.R. McGuire, J.M.D. Coey, A. Gangulee, *J. Appl. Phys.* 49 (1978) 2885.
- [2] J.J. Croat, *J. Appl. Phys.* 53 (1982) 3161.
- [3] R. Politano, J.P. Nozières, R. Perrier, F.P. Missell, *IEEE Trans. Magn.* 29 (1993) 2761.
- [4] K.G. Knoch, G. Schneider, J. Fidler, E.Th. Henig, H. Kronmüller, *IEEE Trans. Magn.* 25 (1989) 3426.
- [5] A. Inoue, T. Zhang, A. Takeuchi, *Sci. Rep. RITU A* 44 (1997) 261.
- [6] A. Inoue, T. Zhang, A. Takeuchi, *IEEE Trans. Magn.* 33 (1997) 3814.
- [7] H. Chiriac, N. Lupu, *Sci. Technol. Adv. Mater.* (accepted).
- [8] R.J. Ortega-Hertogs, PhD thesis, Royal institute of Technology, Stockholm, 2000.
- [9] E. Matsubara, T. Zhang, A. Inoue, *Sci. Rep. RITU A* 43 (1997) 83.
- [10] K. Moorjani, J.M.D. Coey, *Magnetic Glasses*, Elsevier, Amsterdam, 1984.
- [11] J.M.D. Coey, *J. Appl. Phys.* 49 (1978) 1646.
- [12] K.H. Fisher, J.A. Hertz, *Spin Glasses*, Cambridge University, Cambridge, 1993.
- [13] H. Chiriac, N. Lupu, K.V. Rao, *Scr. Mater.* (accepted).